Digest Journal of Nanomaterials and Biostructures Vol. 20, No. 2, April - June 2025, p. 545 - 558

Enhanced mechanical properties and antimicrobial performance of TC4 titanium alloy via surface nanocrystallization and gas nitriding

H. Zheng [a], X. You [a], J. Zhang [b], F. Liu [a], C. Lou [a,*]
[a] *School of Materials Science and Engineering, Shenyang Ligong University,*
Shenyang 110159, China
[b] *Qingdao Choho Industrial Co., Ltd., Qingdao, 266799, China*

The influences of surface nanocrystallization and gas nitriding on the antimicrobial and mechanical properties of TC4 titanium alloy was invesigated in this study. Specimens were treated with shot peening under varying parameter settings, followed by gas nitriding. XRD, SEM, and microhardness testing were used for characterization. Results show that shot peening refines surface grains to the nanoscale, forming a gradient deformation layer and significantly enhancing surface hardness. Gas nitriding of shot-peened samples produces a thicker nitride layer and higher surface hardness compared to untreated samples. However, antimicrobial tests reveal no significant improvement in bactericidal rates. The study concludes that shot peening and gas nitriding significantly enhance the mechanical properties of TC4 titanium alloy and contribute to an improvement in its antimicrobial performance.

(Received February 24, 2025; Accepted May 16, 2025)

Keywords: TC4 titanium alloy, Surface nanocrystallization, Gas nitriding,
Mechanical properties, Antimicrobial performance

1. Introduction

TC4, a representative α+β dual-phase titanium alloy, is extensively employed across aerospace, marine, and biomedical industries, attributable to its exceptional specific strength, exceptional corrosion resistance and fracture toughness [1, 2]. Its low elastic modulus and osseointegration capability make it ideal for orthopedic and dental implants, minimizing stress shielding while promoting bone integration. Despite ISO 10993-certified biocompatibility and high fatigue endurance, TC4 exhibits limited surface hardness and poor tribological performance, restricting its use in wear-critical applications such as articulating joint surfaces [3-5].

To enhance wear resistance, thermochemical treatments like gas nitriding are employed to form hardened ceramic nitride layers [6, 7]. However, prolonged high-temperature exposure risks microstructural degradation. Severe plastic deformation techniques, including controlled shot peening, induce gradient nanostructured surfaces with nanoscale grains, increasing dislocation

---

[*] Corresponding author: chshlou@sylu.edu.cn

https://doi.org/10.15251/DJNB.2025.202.545

density and accelerating nitrogen diffusion kinetics. This synergy enables the formation of thicker nitride layers at reduced temperatures, preserving bulk mechanical properties while optimizing surface hardness [8, 9].

In this study, TC4 titanium alloy was subjected to shot peening to induce surface plastic deformation and form a nanocrystalline layer with a thickness of several micrometers. The optimal shot peening process parameters was determined by analyzing the cross-sectional microhardness before and after treatment. The treated samples were then gas nitrided, and by adjusting the nitriding parameters, a gradient nitride layer was formed on the TC4 surface. The effects of this surface nitriding process on the antimicrobial and mechanical properties were subsequently investigated.

2. Experimental details

The TC4 specimens were precision-sectioned into rectangular blocks measuring 25 mm × 20 mm × 5 mm using electrical discharge machining. A designated working surface was mechanically ground through sequential abrasive polishing with silicon carbide papers (grit sizes: 320→2000) under water-cooled conditions to achieve a mirror finish ($Ra \leq 0.02$ μm). Post-polishing, the samples underwent ultrasonic degreasing in acetone for 15 minutes (40 kHz, 25°C) to remove surface contaminants, followed by immediate drying with oil-free compressed air to prevent oxide formation or particulate adhesion.

The shot-blasting apparatus encompasses an air supply system, a shot-blasting chamber, a projectile recovery system, and ancillary components. Upon ejection of high-pressure gas from the nozzle, a low-pressure cavity forms, which induces the aspiration of cast steel shot from the recovery device into the nozzle. The shot is then propelled by high-velocity gas to impinge upon the specimen surface. The shot-blasting chamber is hermetically sealed and equipped with an exhaust fan to capture dust generated during the experimental process, thus reducing environmental contamination.

The shot-blasting pressure of the equipment was configured at 0.8 MPa, a 5 cm vertical gap was maintained between the nozzle and the specimen surface. The shot-blasting experiments were conducted using cast steel shot with diameters of 0.2 mm, 0.3 mm, and 0.4 mm, respectively. The experiments employed a pressure of 0.8 MPa, with durations varying at 10, 20, 30, and 40 minutes [10].

The phase composition of the specimen was analyzed using a Rigaku Ultima IV X-ray diffractometer. The experiments employed a Cu target with the $K\alpha 1$ characteristic spectral line ($\lambda = 1.54056$ Å). The scanning parameters were set to a speed of 2°/min and a 2θ range of 30° to 90°.

The nitride layer formed after the nitriding process was analyzed using a Hitachi S-3400N scanning electron microscope at a magnification of 3000×. The EDS energy spectrometer, integrated with the microscope, was used to conduct quantitative analysis of the elemental composition within the nitride layer of the samples.

The microhardness of the deformed layer cross-section in the sample was measured using a Vickers microhardness tester (HV-5000) after shot peening. The tests were performed at a load of 5 kg with a 30-second dwell time. Measurements began at a depth of approximately 30 μm from the surface and were taken at 30 μm intervals, concluding at 300 μm. Each sample featured three rows of test points, and the hardness values at each depth were calculated as the average of the three measurements.

In accordance with the antimicrobial test method stipulated in the GB/T 31402-2015 standard, a qualitative analysis of the antimicrobial effect was conducted. During the experiment, the bacterial solution was initially diluted to a concentration of 5.0 × 10^5 CFU/mL. Subsequently, 2 μL of this diluted bacterial solution was inoculated onto the surface of samples. The bacterial solution was initially diluted to a concentration of 5.0 × 10^5 CFU/mL. A 2 μL aliquot of the diluted solution was then inoculated onto the sample surface. The inoculated samples were covered with a polyethylene film and incubated for 24 hours in a temperature- and humidity-controlled chamber. After incubation, the bacterial solution was eluted, diluted, and counted. As a control, 2 μL of the undiluted bacterial solution (5.0 × 10^5 CFU/mL) was directly plated onto an agar culture dish. The experimental groups consisted of the following samples: the original TC4 titanium alloy sample, the 750°C-12h nitrided sample without shot peening, and the nitrided sample after shot peening at 750°C-12h, respectively [11].

3. Results and discussion

3.1. Phase composition analysis of surface nanocrystallizated TC4

Figure 1 presents the X-ray diffraction (XRD) patterns of TC4 titanium alloy samples subjected to multiple shot peening parameters. As shown in the Figure 1(a), the XRD spectrum of the untreated sample exhibits prominent diffraction peaks corresponding to the α-Ti phase, along with a relatively minor presence of β-Ti (110) diffraction peaks. Upon undergoing different shot peening processes, the diffraction peaks associated with the α-Ti phase undergo significant broadening. In Figure 1(b), after shot peening with projectiles of different diameters for a duration of 20 minutes, the X-ray diffraction peaks on the sample surfaces also show broadening, which suggests that the surface grains exhibit a refined structure.

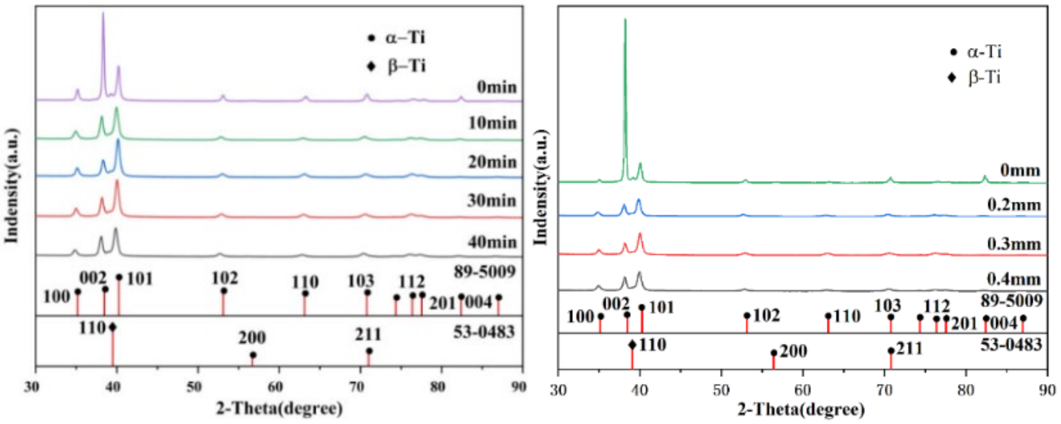

Fig. 1. XRD comparison of TC4 specimens under different shot peening parameters: (a) Shot size fixed at 0.2 mm with varying durations, (b) Varying shot sizes with a fixed shot peening time of 20 minutes.

Due to the overlapping of diffraction peaks caused by peak broadening, to eliminate interference, only the grain sizes of the α (100), α (102), and α (110) crystal planes were calculated when determining the grain size, and the average value was obtained.

The results indicate that after shot peening treatments of varying durations, the grain size on the sample surfaces is significantly reduced [12]. Additionally, the β (110) diffraction peak is observed to gradually diminish with increasing shot peening time. This phenomenon could be due to the weaker diffraction peak of the β (110) crystal plane, whose intensity continues to decrease following peak broadening. In contrast, the diffraction peaks of the adjacent α (002) and α (101) crystal planes are more intense, and after broadening, these peaks effectively mask the diffraction peak of the β (110) crystal plane.

As shown in Figure 2(a), the surface grains of the samples underwent substantial refinement following distinct shot peening processes. After a treatment duration of 10 minutes, the grain size was reduced to the nanoscale, reaching approximately 12.5 nm. Prolonging the treatment time to 20 minutes did not result in a substantial variation in grain sizes, indicating that the grain size had stabilized. while as illustrated in Figure 2(b), the grain size tended to decrease with a reduction in shot diameter, with the smallest grain size being achieved with a shot diameter of 0.2 mm. The shot peening process induces substantial surface plastic deformation of the sample, generating high levels of strain. Due to the strain increases, various slip systems are activated, contributing to the refinement of the grain structure.

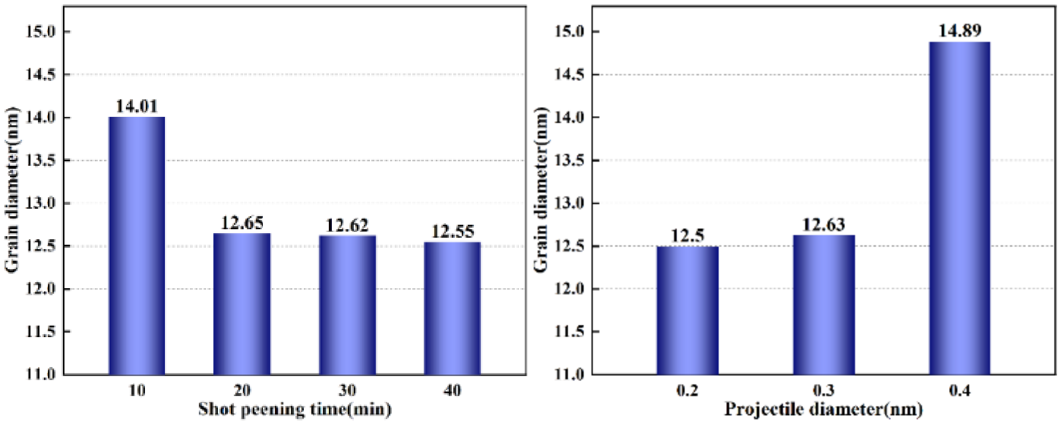

Fig. 2. Comparison of the surface grain size of TC4 specimens subjected to different shot peening parameters: (a) Shot peening is performed using 0.2 mm projectiles, (b) The projectile size varies, while the shot peening time is fixed at 20 minutes.

Due to the hexagonal close-packed (hcp) structure of α-Ti, twinning deformation occurs predominantly at low strain levels. With the accumulation of plastic strain, dislocation generation results in lamellar structure formation with small angular orientation deviations, thereby causing grain subdivision [13,14]. Upon reaching a certain strain level, dislocations reorganize to minimize system energy. In addition, in body-centered cubic β-Ti, dislocation slip is the primary form of plastic deformation. As the shot peening time is extended, the strain gradually increases, leading to an increase in dislocation density at the α-Ti and β-Ti phase interfaces [15]. The densities of dislocation tangles (DT) and dislocation walls (DW) are significantly enhanced. Concurrently, subgrain boundaries progressively form and evolve into high-angle grain boundaries characteristic of nanograins. Under this mechanism, the grain size of the samples undergoes progressive refinement following shot peening. When the grains are refined to a certain extent, a balance between the generation and annihilation of dislocations occurs, resulting in the stabilization of grain size changes.

3.2. Microstructure of the cross-section of surface nanocrystallized TC4

The deformation layer's microstructure observed in cross-sectional TC4 samples following 0.2 mm diameter shot peening under varied processing times is demonstrated in Figure 3. It can be observed that after shot peening, the surface grains are elongated, forming a sheared layer, while the substrate exhibits no significant deformation characteristics. The black line in the figure delineates the boundary between the deformation layer and the substrate. As illustrated in Figure 3, when the shot peening time is 10 minutes, the deformation layer thickness is approximately 12 μm. Increasing the time to 20 minutes raises the thickness to 20 μm.

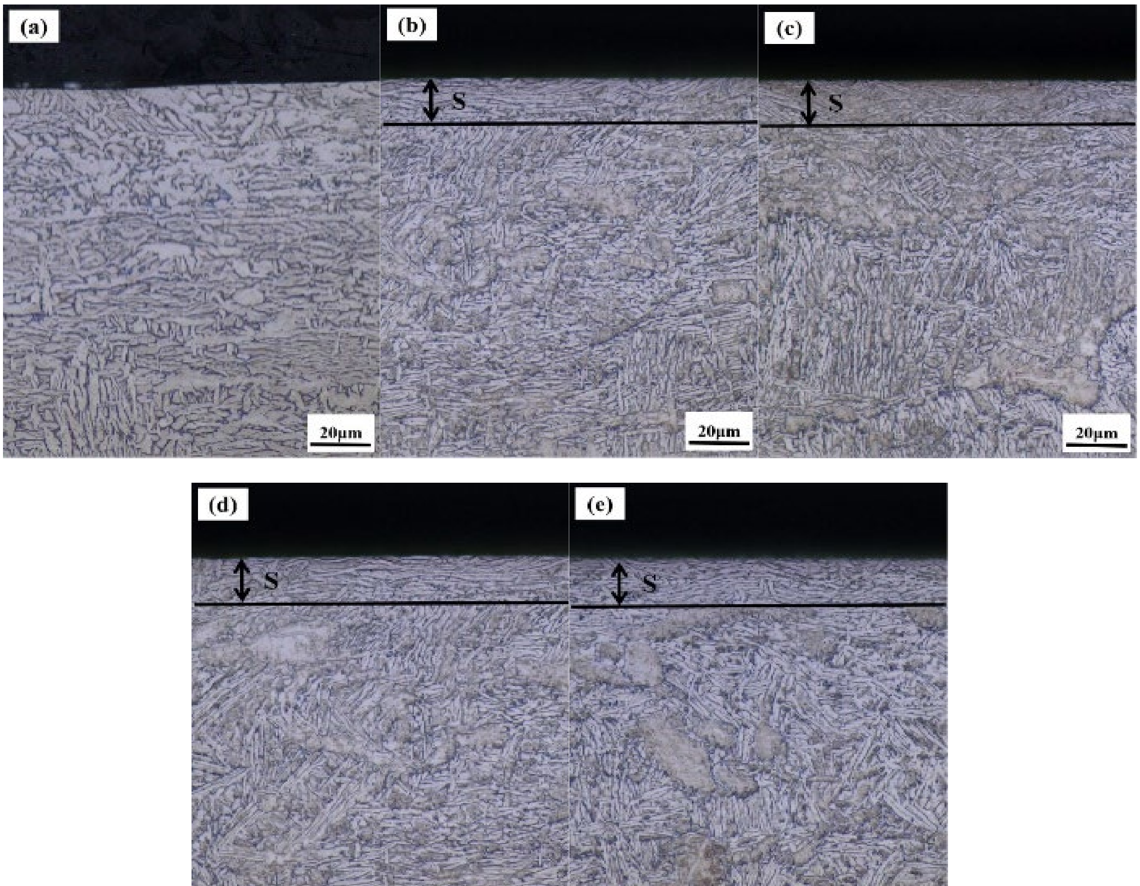

Fig. 3. Microstructure of longitudinal sections under different shot peening durations with 0.2 mm projectiles: (a) 0 min,(b) 10 min, (c) 20 min, (d) 30 min and (e) 40 min.

Further prolonging the treatment results in minimal growth, with the thickness stabilizing around 21 µm. This demonstrates that the deformation layer thickness reaches saturation near 20 µm after 20 minutes of shot peening.

Figure 4 displays the cross-sectional microstructure of the deformation layer in TC4 specimens subjected to 20 minute shot peening using varying shot diameters.The deformation layer thickness measures approximately 20 µm for a shot diameter of 0.2 mm, decreases to 17 µm at 0.3 mm, and further reduces to 12 µm when the shot diameter increases to 0.4 mm. This demonstrates that reducing the shot diameter increases the deformation layer thickness.

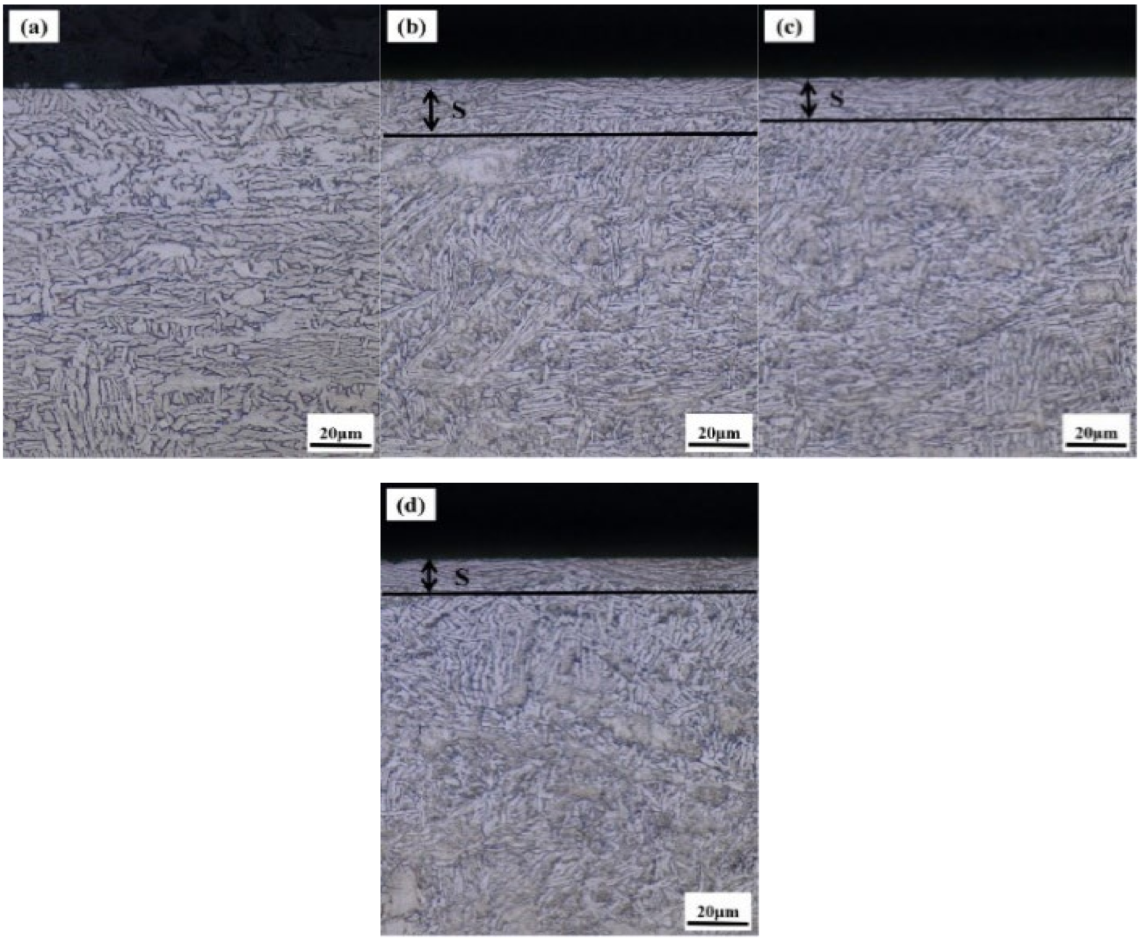

Fig. 4. Microstructure of longitudinal sections with varying projectile sizes under a shot peening duration of 10 minutes: (a) 0 mm, (b) 0.2 mm, (c) 0.3 mm and (c) 0.4 mm.

3.3. Cross-sectional hardness distribution of surface nanocrystallized TC4

Microhardness distribution in longitudinal sections of TC4 specimens under varying shot peening parameters is illustrated in Figure 5. From Figure 5(a), it can be observed that the hardness of the annealed TC4 titanium alloy substrate is 320-330HV. Following 10 minutes of shot peening, the surface hardness escalates to 420HV, reaching 455HV after 20 minutes. With shot peening durations extended to 30 and 40 minutes, the surface hardness increases to 457HV and 475HV, respectively. This indicates that surface nanocrystallization treatment increase visibly the surface hardness of the samples. However, when the surface grains are refined to a stable stage, the increase in surface hardness with increased shot peening time gradually decreases, indicating that further extension of shot peening time can have a negligible effect on the improvement of microhardness [16].

From Figure 5(b), that when the sample surface is bombarded for 20 minutes with shots of diameters 0.2 mm, 0.3 mm, and 0.4 mm, the maximum surface hardness occurs with a 0.2 mm shot diameter, while the minimum hardness corresponds to a 0.4 mm diameter. However, relative to the substrate hardness, the surface hardness of samples bombarded with shots of all three diameters for 20 minutes shows a significant increase. This phenomenon can be attributed to the high-speed impact of shots on the metal surface generating indentations and inducing residual compressive stress, thereby enhancing the surface hardness. Under the same shot peening pressure, shots with less mass have a higher impact velocity, resulting in a greater impact force on the sample surface, introducing more residual compressive stress. The deeper the indentations formed on the surface, the higher the degree of hardening achieved.

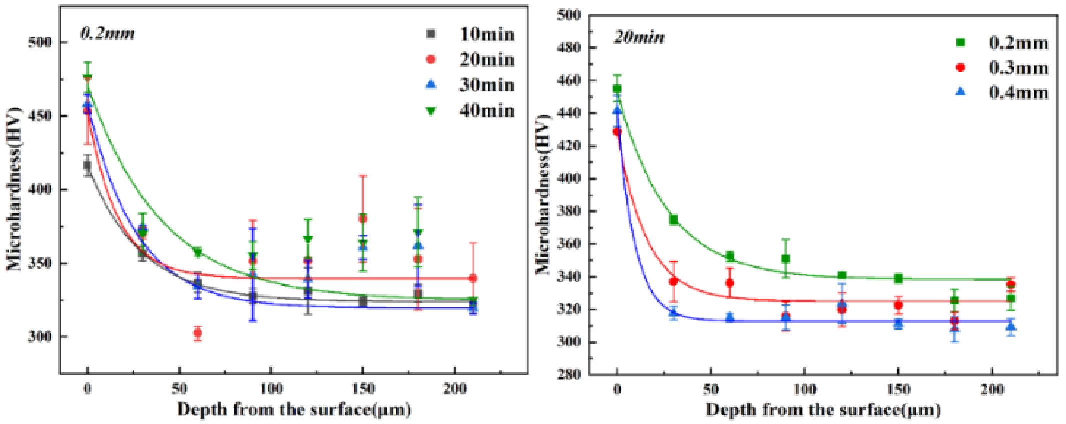

Fig. 5. Microhardness distribution in longitudinal sections of TC4 specimens under distinct shot peening parameters: (a) Time-dependent peening with 0.2 mm projectiles, (b) Projectile size variations under a fixed 20 min peening duration.

It can be observed that the samples processed with 0.2 mm shots for 30 and 40 minutes achieve a stabilized surface grain size. However, the sample peened for 40 min shows a continued increase in surface hardness. The grain size only accounted for α-Ti in the matrix and did not include the secondary phase β-Ti, which may indicate that the refinement of the two phases to a stable stage is not synchronized. After the α-Ti grain size stabilizes, β-Ti may continue to deform during subsequent shot peening processes.

Research has indicated that after α-Ti grains are refined to a stable state and strain continues to increase, dislocations within the grains do not accumulate further but instead undergo rotational recrystallization, with dislocations migrating to grain boundaries and small-angle grain boundaries progressively rotating into large-angle ones [17]. This is significantly different from the dislocation mechanism at the grain boundaries of β-phase grains. Although the original β-Ti grains have become nanograins, they retain abundant dislocations internally. The movement of dislocations can continue to divide β-phase nanograins, reducing their size. In other words, when α grains are refined to nanoscale dimensions, β-phase grains are also refined to the nanoscale. Due to the high density of dislocations within β-phase grains, these grains can continue to be refined to smaller diameters through dislocation motion [18]. The increase in surface hardness observed in samples subjected to 40 min of shot peening with 0.2 mm diameter shot may be attributed to the progressive refinement of the β phase.

3.4. Gas nitriding treatment of surface nanocrystallized TC4

Figure 6 presents the X-ray diffraction spectra of TC4 titanium alloy, comparing its structure before and after optimal shot peening pretreatment under nitriding conditionsof 750°C-10h, 750°C-12h, and 800°C-10h. It can be observed that both the untreated samples and those subjected to shot peening treatment exhibit TiN, Ti_2N, and nitrogen solid solution phases in α-Ti on the surface. The difference lies in the detection of faint Ti_2O diffraction peaks on the surface of the samples after shot peening and nitriding treatment.

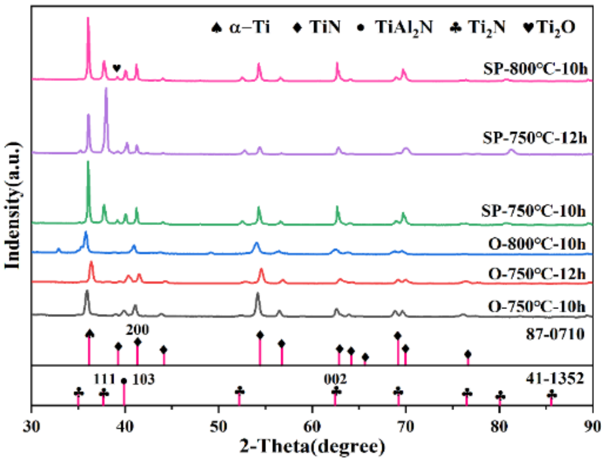

Fig. 6. XRD patterns of TC4 specimen surface under different nitriding processes.

This may be due to the higher activity of the nanostructured grains formed after shot peening, which makes the samples more likely to combine with oxygen during the nitriding process. Moreover, the nanostructured grain structure facilitates the diffusion of nitrogen atoms, thereby promoting the formation of nitrides and enhancing the diffraction peaks of nitrides on the surface of shot-peened and nitrided samples. From the diffraction spectra, it can also be observed that increasing the nitriding temperature or extending the nitriding time alters the preferred orientation of nitride growth. TiN primarily grows along the (200) plane, and Ti2N mainly grows along the (002) plane, which is consistent with the findings of other scholars. As the nitriding temperature elevates, the diffraction peak of the (200) plane of TiN will gradually strengthen, leading to the formation of a texture with a preferred orientation of the (200) plane. This texture formed under high-temperature conditions can increase the surface hardness of the nitride layer.

Figure 7 shows the cross-sectional microstructures of TC4 titanium alloy samples with and without optimal shot peening pretreatment, subjected to nitriding at 750 °C for 10 h, 750 °C for 12 h, and 800 °C for 10 h. As shown in Figure 7(d), the part that can be clearly distinguished from the substrate at the upper surface is the nitride layer, and the layer below that without β-Ti present is the α-case [9]. Under the nitriding condition of 750℃-10h, the untreated sample formed a nitride layer of about 4μm, while the sample after shot peening treatment formed a nitride layer of about 7μm; under the nitriding condition of 750℃-12h, the untreated sample formed a nitride layer of about 7μm, while the sample after shot peening treatment formed a nitride layer of about 10μm. Under the nitriding condition of 800℃-10h, the untreated sample formed a nitride layer of about 20μm, and the sample after shot peening treatment also formed a nitride layer of approximately 20μm.

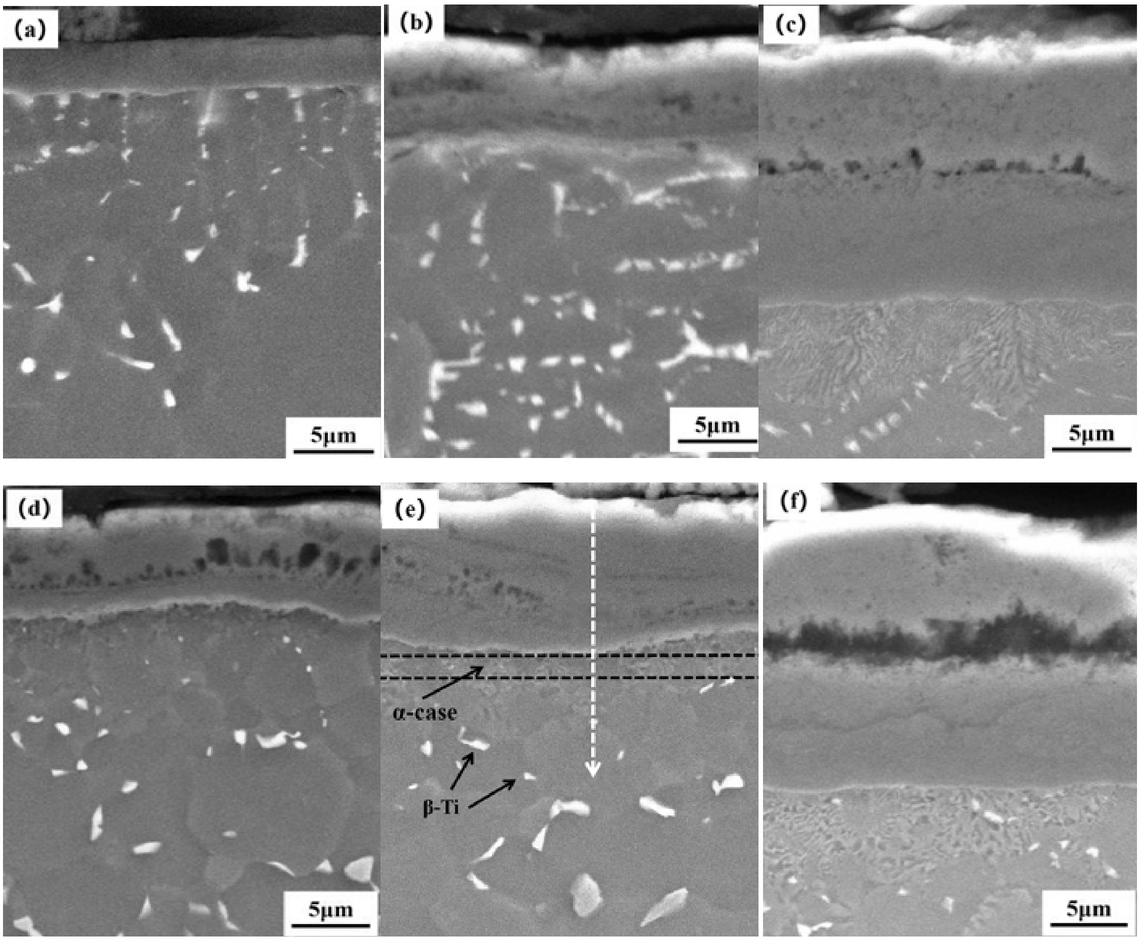

Fig. 7. Cross-sectional microstructure morphology of TC4 specimens under different processes: (a) O-750 ℃-10 h, (b) O-750 ℃-12 h, (c) O-800 ℃-10 h, (d) SP-750 ℃-10 h, (e) SP-750 ℃-12 h and (f) SP-800 ℃-10 h.

Under the conditions of 750℃-10h and 750℃-12h, compared to the nitriding of the original samples, the samples treated with shot peening before nitriding had a significantly thicker nitride layer. However, under the nitriding condition of 800℃-10h, shot peening exhibited negligible influence on the nitride layer thickness.

The nitride layer results from internal nitrogen diffusion followed by chemical interactions with titanium and alloying constituents. Since the nitriding kinetics are relatively weak at 750°C, the nitride layer in the untreated samples is thinner. The surface nanocrystalline layer formed after shot peening introduces more grain boundaries, increases the activity of nitrogen, and provides more diffusion pathways, thus accelerating the diffusion of nitrogen on dislocations and grain boundaries at 750°C, resulting in a thicker nitride layer. At 800°C, the nitriding kinetics are already strong enough, and the driving effect of shot peening on nitriding kinetics is not significant. After nitriding for 10 hours at 800°C, although the samples formed a nitride layer of about 20μm, it can be observed that there are many black pores in the nitride layer, especially in the samples treated with shot peening, where the nitride layer exhibited delamination.

By comparing the conditions at 750°C and 800°C, it can be concluded that due to the high nitriding kinetics at high temperatures, increasing the temperature by 100°C can significantly promote the diffusion of nitrogen. For TC4 titanium alloy treated with shot peening under the condition of 750°C, the high density of dislocations and grain boundaries on the surface enable the formation of a thicker nitride layer that covers the entire surface without peeling off. Shot peening increases the dislocation density in the material surface, promoting the grain size reduction at the top surface with high freedom, thereby accelerating the diffusion of nitrogen.

The elevated concentration of grain boundaries and dislocation networks at the surface facilitates efficient atomic transport, exerting substantial influence on the early phase of gas nitriding—a process governed by interfacial reactions. This results in the formation of a more compact nitride layer following shot peening and nitriding, as opposed to a coarser surface structure. However, when the nitriding temperature reaches 800°C (with the conventional nitriding temperature range for titanium alloys being 780-950°C), the surface nanostructure becomes coarser.

This is because the nanostructure of TC4 alloy maintains its thermal stability up to 750°C [19]. At the high nitriding temperature of 800°C, the diffusion pathways from the high-density grain boundaries of the nanostructure disappear, leading to similar nitriding thicknesses in samples that have undergone shot peening and nitriding compared to those that have not been shot peened. At this temperature, the surface hardness of the nitrided samples without shot peening is substantially enhanced, achieving a value of 1200 HV. In contrast, the surface hardness of the samples subjected to shot peening treatment reaches approximately 1250 HV. The advantage of shot peening is not obvious at 800°C, as nitriding is mainly diffusion-controlled, meaning that increasing the nitriding temperature only increases the diffusion coefficient of N atoms. Microhardness is positively correlated with dislocation density. During the shot peening process, higher stress and high strain rates lead to the generation and multiplication of dislocations, resulting in work hardening and refinement strengthening, which leads to an increase in microhardness. This leads to the gradient change of microhardness as a function of depth after the surface treatment of the TC4 alloy.

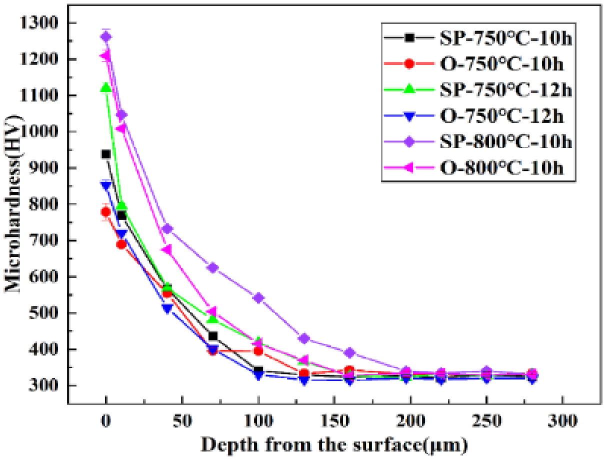

Fig. 8. Cross-sectional microhardness distribution of TC4 specimens under different processes.

The bacterial colony situation of each sample is shown in Figure 9. The results of the antimicrobial experiment are shown in Table 1. As indicated in the table, the bactericidal rate of the TC4 titanium alloy original sample was 12%, the bactericidal rate on the surface of the sample without shot peening and nitriding at 750°C for 12 hours was 8%, while the bactericidal rate on the surface of the sample with shot peening and nitriding under the same conditions reached 25%. It is evident that neither shot peening alone, nitriding alone, nor their combined treatment can significantly enhance the bactericidal rate on the sample surface. Based on the experimental findings, no substances capable of directly killing bacteria were formed or deposited on the sample surfaces following various treatments. However, this does not mean that the samples do not have antimicrobial properties. Studies have shown that after nitriding, The TiN coatings effectively suppress bacterial metabolic activity and significantly limit bacterial adhesion through physical obstruction. Additionally, antibacterial metal ions are gradually released from the TiN coating into the aqueous environment [20,21]. That is, TiN coatings demonstrate inherent antimicrobial properties through their self-limiting release kinetics, creating a protective boundary layer that prevents microbial colonization on medical implants.

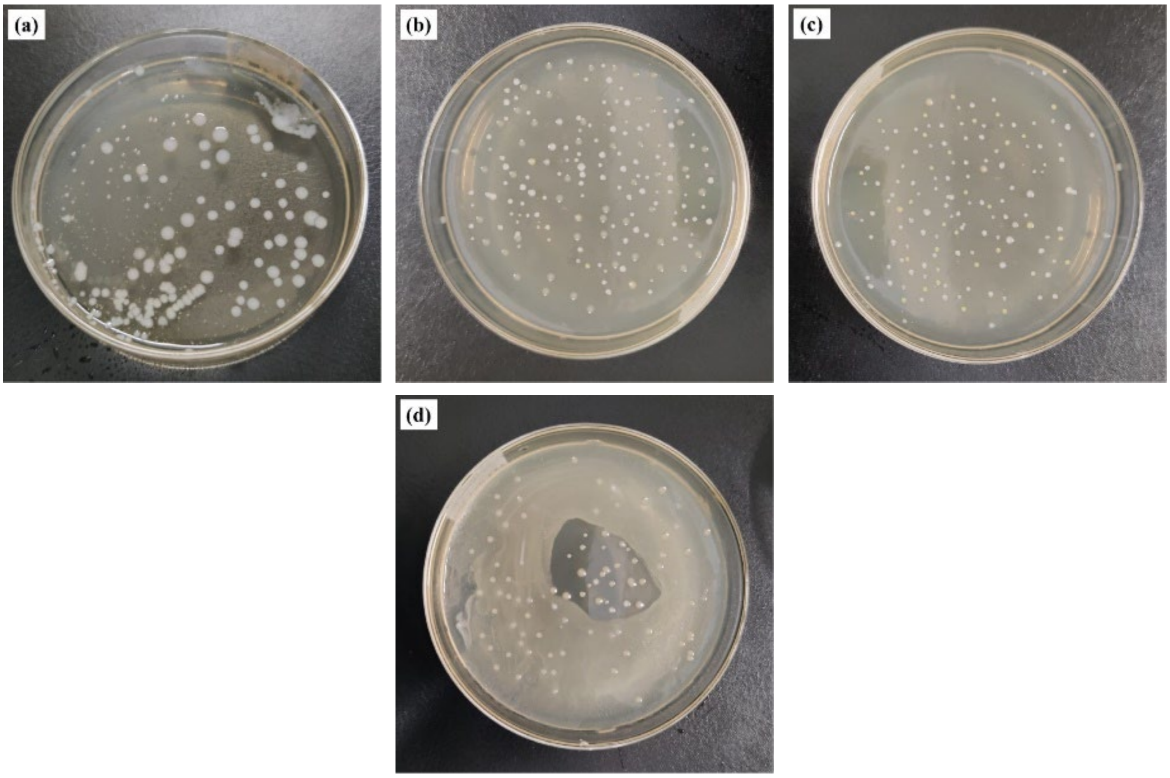

Fig. 9. The number of bacterial colonies: (a) Blank control specimen, (b) Original specimen of TC4, (c) O-750 ℃-12 h and (d)SP-550 ℃-12 h.

Table 1. Results of antimicrobial experiments

Samples	Colony Count (number)	Bactericidal Rate (%)
Blank Control Group	120	0
Original Sample	105	12
Without Shot Peening, Nitriding 750 °C -12 hours	110	8
With Shot Peening, Nitriding 750 °C -12 hours	90	25

4. Conclusions

This study examines the impact of surface nanocrystallization and gas nitriding on the antimicrobial and mechanical properties of TC4 titanium alloy. By performing shot peening with diverse parameters followed by gas nitriding, the following conclusions were drawn:

Shot peening markedly enhances the surface properties of TC4 titanium alloy. When using 0.2 mm balls for 20 minutes of peening, the surface grains are refined to 12.5 nm, resulting in a gradient deformation layer of approximately 21 μm. The microhardness achieves 455 HV, showing a 40% increase compared to the substrate, with the hardness reducing in a stepwise fashion from the surface towards the interior. Prolonged peening time and reduced ball diameter further enhance grain size, deformation layer thickness, and hardness.

The combination of shot peening and gas nitriding significantly strengthens the TC4 titanium alloy. Under medium-temperature nitriding conditions (750℃ for 10-12 hours), the peening pretreatment increases the nitriding layer thickness and surface hardness by 40-80% compared to non-peened samples, with a stepwise hardness distribution. However, high-temperature nitriding at 800℃ for 10 hours weakens the effect of the pretreatment, showing negligible impact on the nitriding layer thickness.

The original TC4 alloy, shot-peened samples, and shot-peened-nitrided samples all exhibit baseline antibacterial properties. Neither shot peening nor gas nitriding significantly improves the antibacterial effectiveness. Despite the mechanical property enhancements, the study concludes that while shot peening and gas nitriding significantly improve the mechanical properties of TC4 titanium alloy, their impact on antibacterial performance remains limited.

References

[1] Debnath S, Ranade R, Wunder S, et al., Dental Materials, 2004, 20(7): 677-86; https://doi.org/10.1016/j.dental.2003.12.001

[2] Wu Q, Miao W S, Gao H J, et al., Nanotechnology Reviews, 2020, 9(1): 259-73; https://doi.org/10.1515/ntrev-2020-0021

[3] Hu R-H, Lim J-K, Materials & Design, 2010,31(5): 2670-5; https://doi.org/10.1016/j.matdes.2009.11.057

[4] Zhao J, Tang J, Zhou W, et al., Surface and Coatings Technology, 2022, 430: 127993; https://doi.org/10.1016/j.surfcoat.2021.127993

[5] Wang Y, Zhang Y, Song G, et al., Materials Today Communications, 2020, 25: 101430; https://doi.org/10.1016/j.mtcomm.2020.101430

[6] Liang J, Liu Q, Li T, et al., Green Chemistry, 2021, 23(8): 2834-67; https://doi.org/10.1039/D0GC03994B

[7] Liu G, Yuan Y, Jiang Z, et al., Materials Research Express, 2020, 7(2): 026401; https://iopscience.iop.org/article/10.1088/2053-1591/ab6e33

[8] Awan A, Pasha R A, Butt M S, et al., Journal of Mechanical Science and Technology, 2020, 34(8): 3227-32; https://doi.org/10.1007/s12206-020-0714-2

[9] He Q, Depaiva J M, Kohlscheen J, et al., International Journal of Refractory Metals and Hard Materials, 2021, 96: 105488; https://doi.org/10.1016/j.ijrmhm.2021.105488

[10] Wang X, Jiang C, Liu T, et al., Surface Topography: Metrology and Properties, 2023, 11(3): 035004; https://doi.org/10.15251/DJNB.2022.174.1151

[11] Lian Z, Zhang J, Wang Y, et al., Journal of Physics: Conference Series; https://doi.org/10.1088/1742-6596/2760/1/012059

[12] Xiao H, Liu X, Lu Q, et al., Journal of Materials Research and Technology, 2022, 19: 2981-90; https://doi.org/10.1016/j.jmrt.2022.06.067

[13] X.D. Ren, W.F. Zhou, F.F. Liu, et al., Applied Surface Science, 2016, 363: 44-49; https://doi.org/10.1016/j.apsusc.2015.11.192

[14] Joshi P, Gupta S, Haque A, et al., Journal of Alloys and Compounds, 2016, 685: 186-193; https://doi.org/10.1016/j.jallcom.2016.05.295

[15] Liu J, Suslov S, Vellore A, et al., Materials Science and Engineering: A, 2018, 736: 335-343; https://doi.org/10.1016/j.msea.2018.08.089

[16] Wang X, Jiang C, Liu T, et al., Surface Topography: Metrology and Properties, 2023, 11(3): 035004; https://doi.org/10.1088/2051-672X/ace467

[17] Liu Y, Li M., Materials Science and Engineering: A, 2016, 669: 7-13; https://doi.org/10.1016/j.msea.2016.05.088

[18] Zhu K, Vassel A, Brisset F, et al., Acta materialia, 2004, 52(14): 4101-10; https://doi.org/10.1016/j.actamat.2004.05.023

[19] Tomasz Moscicki, Rafal Psiuk, Hanna Słomińska, et al., Surface and Coatings Technology,2020, 390: 125689; https://doi.org/10.1016/j.surfcoat.2020.125689

[20] K. A. Whitehead, H. Li, P. J. Kelly, J. Verran , Journal of Adhesion Science and Technology, 2011:25, 2299-2315; https://doi.org/10.1163/016942411X574970

[21] M.A. Hussein, N.K. Ankah, A.M. Kumar, et al., Ceramics International, 2020, 46(11): 18573-18583; https://doi.org/10.1016/j.ceramint.2020.04.164